JOURNAL OF MATERIALS SCIENCE 28 (1993) 6371–6380

Interaction of iron–nickel alloys with liquid aluminium

Part I *Dissolution Kinetics*

V. I. DYBKOV
Institut Problem Materialoznavstva, Kiev 252180, Ukraine

The dissolution of Fe–Ni alloys containing 90 to 5 mass % Fe in liquid aluminium at 700 °C was found by the rotating-disc technique to be non-selective and diffusion controlled. Experimentally determined values of the saturation concentration (solubility), c_s, of iron and nickel from Fe–Ni alloys in the aluminium melt are presented. A dependence of the total iron and nickel concentration, c_{total}, in the saturated melt upon the iron content C_{Fe}, in initial Fe–Ni alloys could well be described by the linear equations: $c_{total} = 7.51 - 0.054C_{Fe}$ at $90\% < C_{Fe} < 28\%$ and $c_{total} = 11.0 - 0.19C_{Fe}$ at $28\% < C_{Fe} < 5\%$. Considerable deviations of the concentration–time relationships from the Nernst–Shchukarev equation were revealed. The value of the dissolution rate constant was found to decrease by about 20 to 30% in the 0 to $c_s/2$ iron or nickel concentration range. Accordingly, the decrease in value of the iron and nickel diffusion coefficient from an Fe–Ni alloy into liquid aluminium was 25 to 40%. For a 90% Fe–10% Ni alloy the value of the diffusion coefficient tends, with increasing iron and nickel concentration in the melt, to the value of the diffusion coefficient of pure iron in liquid aluminium. For other Fe–Ni alloys investigated, these values are less than or close to the diffusion coefficient of pure nickel in liquid aluminium.

1. Introduction

After wetting the surface of a solid Fe–Ni alloy material by liquid aluminium, two other closely interrelated processes (namely, dissolution of the solid base into the liquid phase and growth of intermetallics at their interface) proceed simultaneously. Besides the scientific interest, both are of importance for technological applications including hot-dip aluminizing and the joining of dissimilar materials.

For the reasons discussed in a previous work [1], the dissolution of an Fe–Ni alloy in liquid aluminium may equally be expected to be selective (enhanced transition of one of the two elements from the alloy into the aluminium melt) or non-selective (equal rates of transition of iron and nickel from the alloy into the aluminium melt) in nature. The results of studying the dissolution kinetics of Fe–Ni alloys containing 90 to 5 mass % Fe in liquid aluminium at 700 °C are presented in this paper. (All values for content or concentration are given in mass %. The most important values are followed by their 0.95 confidence limits.)

Experimental data on the phase composition, structure and growth kinetics of intermetallic layers will be presented separately.

2. Experimental procedure

2.1. Materials

High-purity aluminium (99.995% Al), carbonyl iron (99.98% Fe) and electrolytic nickel (99.98% Ni) were used for this investigation.

2.2. Alloy preparation

The Fe–Ni alloys were arc melted from their components in a conventional arc-melting furnace under argon and then cast into a 13 mm inner diameter (i.d.) and 100 mm high massive copper crucible. By inverting the samples between melts and remelting five times, homogeneous alloys could readily be prepared.

2.3. Specimens

Cylindrical specimens, 11.28 ± 0.01 mm diameter and 6 mm high, were machined from the 13 mm diameter alloy rods obtained. The disc surfaces were then ground flat and polished mechanically.

Before the experiment, the alloy specimen was rinsed in ethanol and dried. It was then pressed into a high-purity graphite tube, of 16.0 mm diameter, to protect its lateral surface from the aluminium-melt attack. Therefore, only the disc surface, 1 cm^2 area, dissolved during the run.

In the case of solubility determinations where a greater surface area was desirable to reduce the duration of the runs while the exact instantaneous value was unimportant, cylindrical alloy specimens with unprotected lateral surfaces were used. Their total initial surface area was 3.0 cm^2.

0022–2461

2.4. Specimen characterization

2.4.1. Chemical composition

Samples of shavings obtained after machining the specimens were chemically analysed to determine their iron and nickel contents. Specimen homogeneity was checked using as electron probe microanalyser Jeol-Superprobe 733. As seen from Table I, all three values of the alloy composition obtained by the different methods agree within $\pm$ 0.5%; the deviations from the mean appear to be quite random. Therefore, nominal compositions were used for calculations.

TABLE I Chemical compositions of Fe–Ni alloy specimens

Content of elements (%)					
Fe			Ni		
Nominal	CA[a]	EPMA[b]	Nominal	CA[a]	EPMA[b]
90	89.9	89.8	10	9.7	10.2
75	74.7	75.5	25	24.8	23.5
50	49.3	50.6	50	48.4	49.4
25	25.5	25.5	75	74.9	74.5
20	20.0	20.2	80	79.3	79.8
15	15.3	15.6	85	85.2	84.4
10	10.4	10.5	90	89.5	90.5

[a] Obtained by chemical analysis.
[b] The mean value of three to six electron-probe measurements at different places on the disc surface, the scatter within each specimen being $\pm$ 0.5%.

2.4.2. Phase composition

Microscopic examination of the cross-sections showed the specimens to have one phase. X-ray patterns of polished alloy discs were obtained with a 57.3 mm diameter camera using CuKα or CrKα radiation. The results are presented in Table II. As seen, at room temperature the alloy specimens consisted of the α-phase at Ni contents less than or equal to 25% or the γ-phase at higher Ni contents, in agreement with the available literature data [2–5].

Note that at the temperature chosen in this investigation, 700 °C, all the alloy specimens had austenitic structures. Indeed, even for a 90% Fe–10% Ni alloy

TABLE II X-ray characterization of Fe–Ni alloys

Content of Fe in alloy (%)	*h k l*	*d*-spacing (nm)	$a_{experimental}$ (nm)	$a_{literature}$ [3] (nm)	Phase
90	1 1 0	0.203	0.287	0.2863[a]	α
	2 0 0	0.1435	0.287		
	2 1 1	0.1171	0.287		
	2 2 0	0.1020	0.288		
	3 1 0	0.09080	0.287		
75	1 1 0	0.202	0.286	–	α
	2 0 0	0.1435	0.287		
	2 1 1	0.1166	0.286		
	2 2 0	0.1017	0.288		
	3 1 0	0.09054	0.286		
50	1 1 1	0.205	0.355	0.3587	γ
	2 0 0	0.179	0.358		
	2 2 0	0.1265	0.358		
	3 1 1	0.1082	0.359		
50[b]	1 1 1	0.206	0.357	0.3587	γ
	2 0 0	0.179	0.358		
	2 2 0	0.127	0.359		
	3 1 1	0.1082	0.359		
25	1 1 1	0.205	0.355	0.3554	γ
	2 0 0	0.178	0.356		
	2 2 0	0.1257	0.356		
	3 1 1	0.1071	0.355		
20	1 1 1	0.205	0.355	0.3548	γ
	2 0 0	0.177	0.354		
	2 2 0	0.1252	0.354		
	3 1 1	0.1068	0.355		
15	1 1 1	0.204	0.353	0.3537	γ
	2 0 0	0.177	0.354		
	2 2 0	0.1248	0.353		
	3 1 1	0.1067	0.354		
10	1 1 1	0.203	0.352	0.3527	γ
	2 0 0	0.176	0.352		
	2 2 0	0.1250	0.353		
	3 1 1	0.1066	0.353		

[a] 95% Fe.
[b] Quenched in water from 700 °C after the dissolution run.

the temperature of the $\alpha \rightarrow \gamma$ transformation is reported to be 640 °C [3] or at most 695 °C [2, 4] depending upon the previous heat treatment. As this transformation is diffusionless (martensitic) in nature, its rate is very high. Therefore, the time of specimen preheating (from room temperature to 700 °C) and of temperature equilibration (typically 600 s) appears to be sufficient for the completion of the $\alpha \rightarrow \gamma$ transformation.

2.5. Methods

The experimental procedure did not differ from that described in the previous work [1]. Therefore, only a very brief description is given here.

The experiments were performed mainly by the rotating-disc technique. A special flux was used both to protect the aluminium melt from oxidation and to preheat the specimen to the required temperature. After the temperature had equilibrated, the specimen, rotating at the intended angular speed, was lowered from its position in the middle of the flux melt into the bulk of the liquid aluminium. This was the beginning of the run. The disc was allowed to rotate in the aluminium melt (10 cm^3 volume at 700 °C) for a predetermined period of time. At the end of the run, it was lifted above the melt and cooled in a water bath.

The temperature of the liquid phase was measured by a chromel–alumel thermocouple. During the run, its deviations were 2 to 5 °C.

After cooling, the major portion of the aluminium alloy adhering to the Fe–Ni alloy surface was removed mechanically. The remainder was dissolved in a 10% aqueous solution of NaOH. The alloy specimen was then washed with water and alcohol, dried and weighed to determine its mass loss during dissolution in liquid alumimium.

Samples of the Al–Fe–Ni alloys obtained were analysed to find their iron and nickel contents by photometric methods. The relative error in this determination did not exceed ± 10% for both elements.

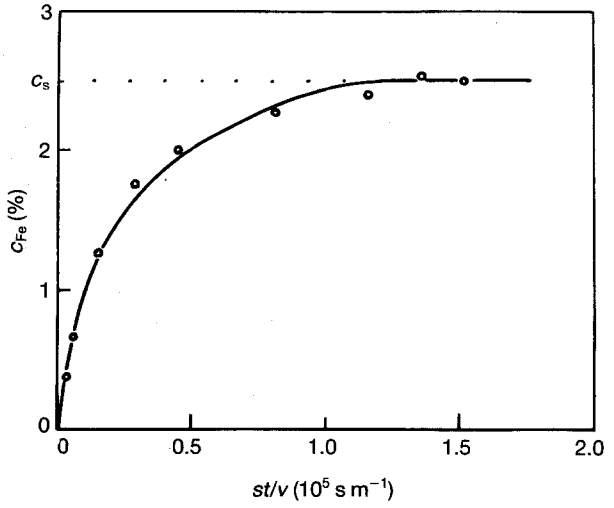

Figure 1 Concentration of iron from a 50% Fe–50% Ni alloy in liquid aluminium plotted against st/v to determine the saturation concentration, c_s. Temperature = 700 °C, rotational speed ω = 24.0 rad s^{-1}.

3. Results and discussion

3.1. Saturation concentration

The Nernst–Shchukarev equation appears to be basic to the understanding of the nature of the dissolution process of any solid in a liquid phase. Its differential form is as follows

$$\frac{dc}{dt} = \frac{k s}{v}(c_s - c) \quad (1)$$

where c is the concentration of the dissolved material in the bulk of the melt or solution (kg m^{-3} or per cent at low values of concentration), t is the time (s), c_s is the saturation concentration or solubility (kg m^{-3} or per cent), k is the dissolution rate constant (m s^{-1}), s is the solid specimen surface area (m^2), and v is the melt volume (m^3).

In the integrated form (for initial conditions, $c = 0$ at $t = 0$) it becomes

$$c = c_s\left[1 - \exp\left(-\frac{kst}{v}\right)\right] \quad (2)$$

TABLE III Concentrations of iron and nickel undergoing dissolution from a 50% Fe–50% Ni alloy into liquid aluminium for temperature = 700 °C, rotational speed ω = 24.0 rad s^{-1}, s/v = 10 m^{-1}

Time (s)	Concentration of elements in aluminium (%)				Ratio[a], c_{Fe}/c_{Ni}, of concentrations in the melt
	Fe		Ni		
	ML[b]	CA[c]	ML[b]	CA[c]	
300	0.41	0.40	0.41	0.39	1.03
600	0.69	0.67	0.69	0.70	0.96
1 500	1.28	1.23	1.28	1.17	1.05
4 500	2.07	1.9	2.07	2.1	0.90
8 100	2.28	2.4	2.28	2.2	1.09
11 700	2.43	2.4	2.43	2.3	1.04
13 500	2.54	2.4	2.54	2.4	1.00
15 000	2.50	2.4	2.54	2.5	0.96

[a] Calculated using the results of chemical analysis of Al–Fe–Ni alloys.
[b] Calculated from mass-loss measurements.
[c] Obtained by chemical analysis of Al–Fe–Ni alloys after the runs.

From these equations it follows that the concentration of the dissolved phase in the liquid tends, with passing time, to a limiting value, c_s, as is the case for Fe–Ni alloys, Fig. 1 and Tables III and IV. At 700 °C, this value is 2.5 % for iron in the Al–Fe binary system and 10.0% for nickel in the Al–Ni binary system (see [1]).

The primary data on the determination of the saturation concentrations of iron and nickel from Fe–Ni alloys in liquid aluminium are presented in Table IV and the final values are listed in Table V.

Note that the dissolution process is non-selective. Indeed, the value of the iron and nickel concentration in the aluminium melt obtained from mass-loss measurements on the assumption of non-selective dissolution of any Fe–Ni alloy in liquid aluminium coincides within the limits of the experimental error with that found by chemical analysis of Al–Fe–Ni alloys after the runs (see Tables III and IV). Non-selectivity of the alloy dissolution in liquid aluminium is also supported by the fact that no appreciable change in solid-base composition (up to a distance of 10 μm from the alloy–aluminium interface) was determined by EPMA. The composition of all specimens after the run remained uniform (within ± 0.5%) throughout their

TABLE IV Determination of the saturation concentration of iron and nickel from Fe–Ni alloys in liquid aluminium for temperature = 700 °C, $s/v < 30\ m^{-1}$

Content of Fe in the alloy (%)	Time (s)	ω (rad s^{-1})	Concentration of elements in aluminium (%)				Ratio, c_{Fe}/c_{Ni}, of concentrations in the melt
			Fe		Ni		
			ML[a]	CA[b]	ML[a]	CA[b]	
90	2700	82.4	2.46	2.25	0.27	0.23	9.7
	3300	54.0	2.36	2.22	0.26	0.27	8.2
	3600	82.4	2.49	2.31	0.28	0.29	8.0
	3600	54.0	2.50	2.25	0.28	0.26	8.7
	4000	54.0	2.47	2.25	0.27	0.27	8.3
80	3000	82.4	2.48	2.41	0.62	0.63	3.8
	3600	82.4	2.49	2.35	0.62	0.70	3.4
	3700	82.4	2.50	2.41	0.63	0.60	4.0
75	3000	82.4	2.65	2.40	0.88	0.86	2.8
	3600	54.0	2.56	2.50	0.85	0.82	3.1
	3600	82.4	2.49	2.27	0.83	0.80	2.8
65	3200	82.4	2.59	2.25	1.39	1.23	1.83
	3600	82.4	2.58	2.42	1.38	1.32	1.83
	4000	82.4	2.53	2.40	1.36	1.26	1.90
60	3000	82.4	2.58	2.34	1.72	1.53	1.52
	3600	82.4	2.58	2.25	1.72	1.65	1.36
	4000	82.4	2.51	2.20	1.67	1.51	1.47
50	2700	32.7	2.42	2.40	2.42	2.30	1.04
	3000	54.0	2.47	2.32	2.47	2.50	0.93
	3600	32.7	2.41	2.30	2.41	2.37	0.97
	3600	54.0	2.59	2.35	2.59	2.50	0.94
	4500	32.7	2.53	2.12	2.53	2.40	0.88
40	3000	82.4	2.21	2.28	3.31	3.37	0.70
	3600	82.4	2.20	2.19	3.31	3.25	0.67
	4000	82.4	2.23	2.16	3.35	3.11	0.69
30	3400	82.4	1.74	1.60	4.05	3.80	0.42
	3600	82.4	1.78	1.70	4.14	3.95	0.43
	4000	82.4	1.75	1.70	4.07	3.84	0.44
25	3000	82.4	1.61	1.51	4.82	4.47	0.34
	3600	54.0	1.60	1.55	4.79	4.40	0.35
	3600	82.4	1.63	1.44	4.90	4.44	0.32
	4500	54.0	1.61	1.40	4.81	4.40	0.32
	4500	82.4	1.60	1.43	4.80	4.43	0.32
20	2700	32.7	1.33	1.30	5.31	5.00	0.26
	3600	32.7	1.35	1.30	5.40	5.10	0.25
	3600	54.0	1.44	1.35	5.76	5.35	0.25
	3600	82.4	1.47	1.27	5.89	5.35	0.24
	4500	54.0	1.48	1.25	5.92	5.40	0.23
	4500	82.4	1.54	1.23	6.17	5.45	0.23
	5400	82.4	1.47	1.22	5.86	5.40	0.23

[a] Calculated from mass-loss measurements.
[b] Obtained from chemical analysis of Al–Fe–Ni alloys after the runs.

TABLE V Values of the saturation concentration (solubility) of iron and nickel from Fe–Ni alloys in liquid aluminium at 700 °C

Content of Fe in alloy (%)	Saturation concentration (solubility) (%)		Total concentration of Fe and Ni in aluminium (%)
	Fe	Ni	
100	2.5 ± 0.1	–	2.5
90	2.5 ± 0.2	0.28 ± 0.02	2.78
80	2.5 ± 0.2	0.63 ± 0.05	3.13
75	2.5 ± 0.2	0.86 ± 0.07	3.36
65	2.5 ± 0.2	1.35 ± 0.08	3.85
60	2.5 ± 0.2	1.67 ± 0.09	4.17
50	2.5 ± 0.5	2.5 ± 0.2	5.0
40	2.2 ± 0.1	3.3 ± 0.1	5.5
30	1.76 ± 0.07	4.0 ± 0.2	5.76
25	1.61 ± 0.05	4.8 ± 0.3	6.41
20	1.44 ± 0.09	5.8 ± 0.4	7.24
15	1.25 ± 0.04	4.1 ± 0.5	8.35
10	0.90 ± 0.04	8.1 ± 0.3	9.0
5	0.51 ± 0.03	9.8 ± 0.2	10.3
0	–	10.0 ± 0.5	10.0

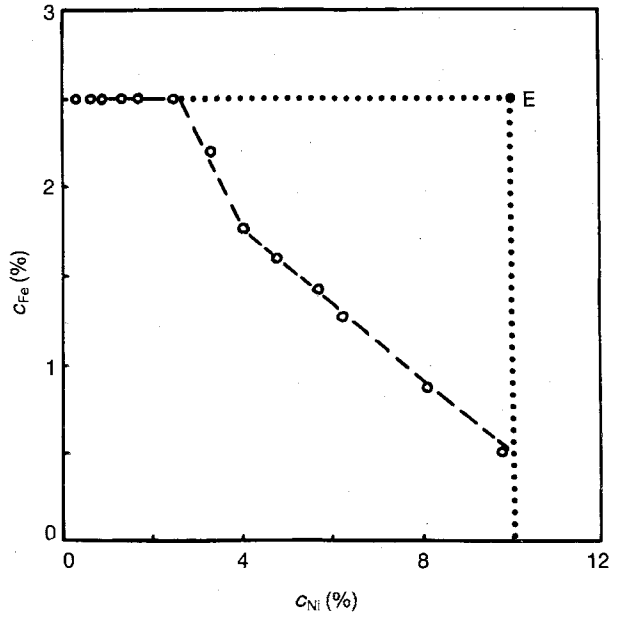

Figure 2 Isothermal-solubility diagram of iron and nickel from Fe–Ni alloys in liquid aluminium at 700 °C.

bulk and corresponded to the composition of the initial alloy.

An isothermal-saturation-concentration (solubility) diagram of iron and nickel from Fe–Ni alloys in liquid aluminium at 700 °C is shown in Fig. 2. It displays a strong mutual influence of the elements on their solubilities in the aluminium melt. In the case of no mutual influence the diagram would be like that shown by the dotted lines, with a eutonic point, E, at 2.5 % Fe and 10.0 % Ni [6]. As seen from Fig. 2 and Table V, the influence of iron on the nickel solubility in the melt is more pronounced than that of nickel on the iron solubility.

A dependence of the total concentration, $c_{total} = C_{Fe} + c_{Ni}$, of iron and nickel from Fe–Ni alloys in the saturated aluminium melt upon the iron content, C_{Fe}, in the initial Fe–Ni alloy is shown in Fig. 3. This dependence could formally be described with good accuracy by the following two straight-line equations:

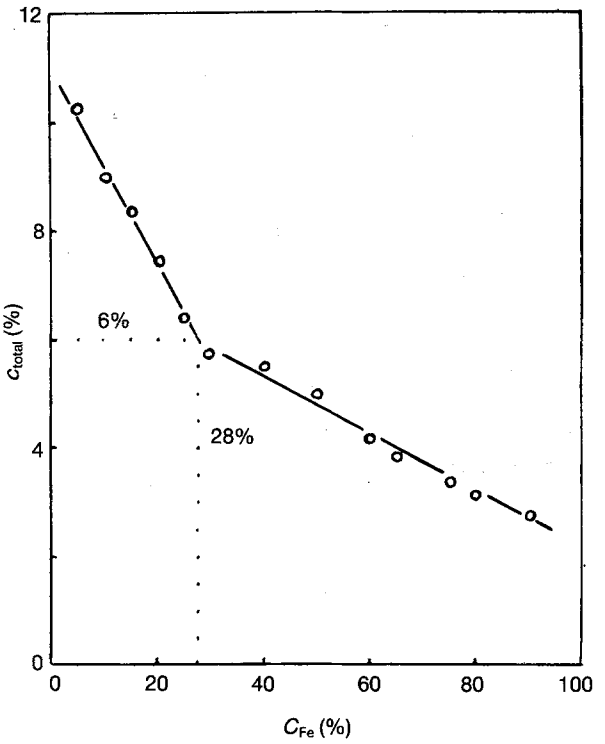

Figure 3 Total concentration of iron and nickel in liquid aluminium at 700 °C plotted against the iron content of the initial Fe–Ni alloys.

$$c_{total} = 7.51 - 0.054C_{Fe} \quad (\text{at } 90\% < C_{Fe} < 28\%) \tag{3}$$

and

$$c_{total} = 11.0 - 0.19C_{Fe} \quad (\text{at } 28\% < C_{Fe} < 5\%) \tag{4}$$

Equations 3 and 4 were obtained by the least-squares-fit method. The correlation coefficient is 0.992 for the first line and 0.995 for the second. Deviations of c_{total} calculated according to these equations from experimental values do not exceed ± 0.2%. The lines intersect at $c_{total} = 6\%$ and $C_{Fe} = 28\%$. Note that the saturation concentrations of iron and nickel from any commercial Fe–Ni alloy can readily be found using Equations 3 and 4 and its Fe content.

3.2. Dissolution rate constant

In addition to the saturation concentration (solubility), c_s, another important characteristic of the dissolution process is the dissolution rate constant, k. To find its exact values, the initial parts of the dissolution curves were thoroughly investigated. The experimental data obtained for a 50% Fe–50% Ni alloy are shown in Figs 4 and 5 and Table VI.

As seen, noticeable deviations from the Nernst–Shchukarev equation are observed in the case under consideration since the value of the dissolution rate constant decreases with increasing dipping time. The reason is probably again a mutual influence of iron and nickel on the rate of their transition across

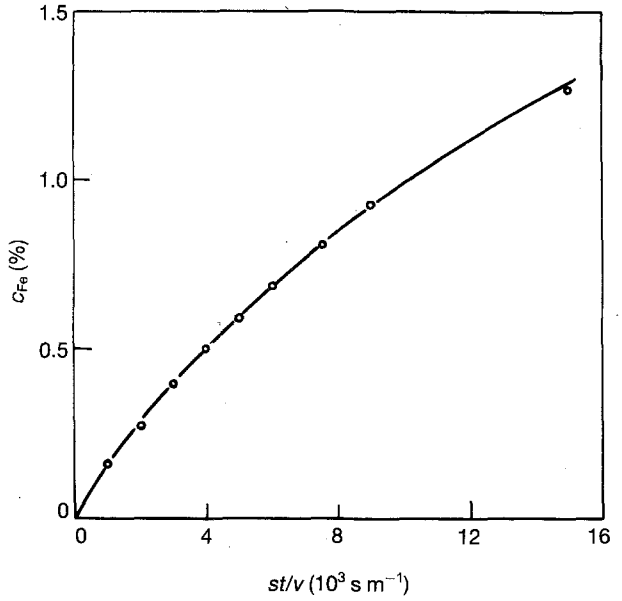

Figure 4 Concentration of iron from a 50% Fe–50% Ni alloy in liquid aluminium plotted against st/v. Temperature = 700 °C, $\omega = 24.0$ rad s^{-1}, $s/v = 10$ m^{-1}.

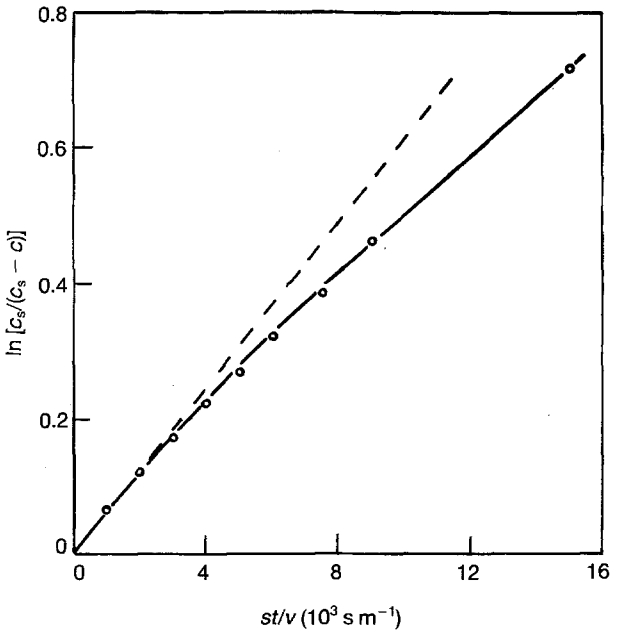

Figure 5 A plot of ln $[c_s/(c_s-c)]$ against st/v for the data of Fig. 4.

the diffusion boundary layer at the solid–liquid interface. Indeed, the dissolution rate constant, k, is related to the diffusion coefficient, D, of the solute atoms by the Nernst equation

$$k = D/\delta \tag{5}$$

where δ is the thickness of the diffusion boundary layer (m).

As the mean value of solute concentration in the diffusion boundary layer changes with passing time from $c_s/2$ at $t = 0$ up to c_s at $t \to \infty$, a decrease in D may be expected if the iron and nickel atoms mutually hinder their movement across the layer. This decrease cannot be large, however, since even for Ni-rich alloys the concentration range (from about 5% to 10%) is too narrow to cause a great change in the value of the diffusion coefficient. In fact, in the 100 to 1500 s time range (up to $c = c_s/2$) the dissolution rate constant decreases by less than 30% (See Table VI).

3.3. The effect of rotational speeds on the dissolution rate constant

For a rotating disc, the dissolution rate constant, k, is related to the angular speed of rotation, ω, by the following equation given by Levich [7]

$$k = 0.62 D^{2/3} \nu^{-1/6} \omega^{1/2} \tag{6}$$

where ν is the kinematic viscosity of the liquid phase (m^2 s^{-1}). At low values of the Schmidt number, $Sc = \nu/D$, the Kassner equation which holds for $Sc > 4$ is preferable

$$k = 0.554 I^{-1} D^{2/3} \nu^{-1/6} \omega^{1/2} \tag{7}$$

where I is a function of Sc [8].

In addition to the runs performed at a rotational speed of 24.0 rad s^{-1}, the dissolution rates of a 50% Fe–50% Ni alloy in liquid aluminium were also measured at the angular speeds of the disc rotation 6.45, 9.00, 15.3, 32.7, 54.0 and 82.4 rad s^{-1}. The concentrations of iron from a 50% Fe–50% Ni alloy into the melt are plotted against st/v for these seven rotational speeds in Fig. 6. Corresponding values of the dissolution rate constant, k, are listed in Table VII. Again, a decrease in k-values with increasing dipping time is seen.

While the dissolution rate constant does not remain constant, the $k - \omega^{1/2}$ dependence is nevertheless linear if all k-values are measured at the same iron and nickel concentration in the melt for all rotational speeds, Fig. 7. This is evidence of the diffusion-controlled character of the alloy dissolution in liquid aluminium.

3.4. Dissolution rates of Fe–Ni alloys of different compositions

A tendency towards decreasing the dissolution rate constant with increasing dipping time and consequently the concentration of iron and nickel is observed for all the Fe–Ni alloys investigated, Table VIII. A decrease in k-values is clearly most pronounced at small times. At high times, the dissolution rate constant tends to a limiting value which is characteristic of the saturated melt.

Note that under the same conditions the dissolution rate constant of any Fe–Ni alloy in liquid aluminium (see Tables VI and VIII) is greater than that of pure iron or an 18Cr–10Ni stainless steel. For example, at a temperature of 700 °C and a rotational speed of 24.0 rad s^{-1} its value is 3.8×10^{-5} m s^{-1} for pure iron [9] and 4.8×10^{-5} m s^{-1} for an 18Cr–10Ni stainless steel [1]. Both values are less than those listed in Table VI and VIII. This means that the Fe–Ni alloys are less resistant to the liquid-aluminium attack than these two materials.

TABLE VI Experimental data on the dissolution kinetics of a 50% Fe–50% Ni alloy in liquid aluminium, for temperature = 700 °C, $\omega = 24.0$ rad s^{-1}, $s/v = 10$ m^{-1}

Time (s)	Concentration of elements in aluminium (%)				$\ln [c_s/(c_s - c)]$	$k(10^{-5}$ m s$^{-1})$
	Fe		Ni			
	ML[a]	CA[b]	ML[a]	CA[b]		
100	0.16	0.16	0.16	0.16	0.0661	6.6
200	0.28	0.31	0.28	0.26	0.1188	5.9
300	0.40	0.39	0.40	0.40	0.1744	5.8
400	0.50	0.44	0.50	0.50	0.2231	5.6
500	0.59	0.54	0.59	0.59	0.2692	5.4
600	0.69	0.67	0.69	0.70	0.3229	5.4
750	0.81	0.73	0.81	0.74	0.3916	5.2
900	0.93	0.86	0.93	0.85	0.4652	5.2
1500	1.28	1.23	1.28	1.17	0.7174	4.8

[a] Calculated from mass-loss measurements.
[b] Obtained by chemical analysis of Al–Fe–Ni alloys after the runs.

TABLE VII Experimental data on the dissolution kinetics of a 50% Fe–50% Ni alloy in liquid aluminium at different angular speeds of the disc rotation, for temperature = 700 °C, $s/v = 10$ m^{-1}

ω (rad s^{-1})	Time (s)	Concentration of Fe in aluminium (%)	$\ln[c_s/(c_s - c)]$	$k(10^{-5}$ m s$^{-1})$
6.45	600	0.34	0.1462	2.4
	900	0.45	0.1984	2.2
	1200	0.60	0.2744	2.3
	1500	0.61	0.2797	1.9
	1800	0.69	0.3230	1.8
	2400	0.80	0.3857	1.6
9.00	300	0.24	0.1009	3.4
	600	0.41	0.1791	3.0
	900	0.56	0.2536	2.8
	1200	0.70	0.3285	2.7
	1500	0.84	0.4095	2.7
	1800	0.91	0.4526	2.5
15.3	300	0.32	0.1371	4.5
	450	0.45	0.1984	4.4
	600	0.58	0.2640	4.4
	900	0.72	0.3397	3.8
	1200	0.86	0.4216	3.5
	1500	1.03	0.5310	3.5
32.7	200	0.33	0.1416	7.1
	300	0.44	0.1936	6.5
	450	0.60	0.2744	6.1
	600	0.74	0.3509	5.8
	750	0.86	0.4216	5.6
	900	0.98	0.4976	5.5
54.0	200	0.44	0.1936	9.6
	300	0.58	0.2640	8.8
	450	0.78	0.3740	8.3
	600	1.00	0.5108	8.5
	750	1.09	0.5727	7.6
	800	1.18	0.6387	8.0
82.4	150	0.41	0.1791	11.9
	300	0.70	0.3285	11.0
	350	0.80	0.3587	11.0
	450	0.94	0.4716	10.5
	600	1.19	0.6463	10.8
	750	1.40	0.8210	10.9

3.5. Diffusion coefficients

The diffusion coefficient of the iron and nickel atoms from the Fe–Ni alloys investigated across the diffusion boundary layer into the bulk of liquid aluminium could clearly be estimated using Equations 6 and 7 and known values of k, v and ω. However, two problems arose. The first was the lack of necessary data on the viscosity of the aluminium melts containing iron

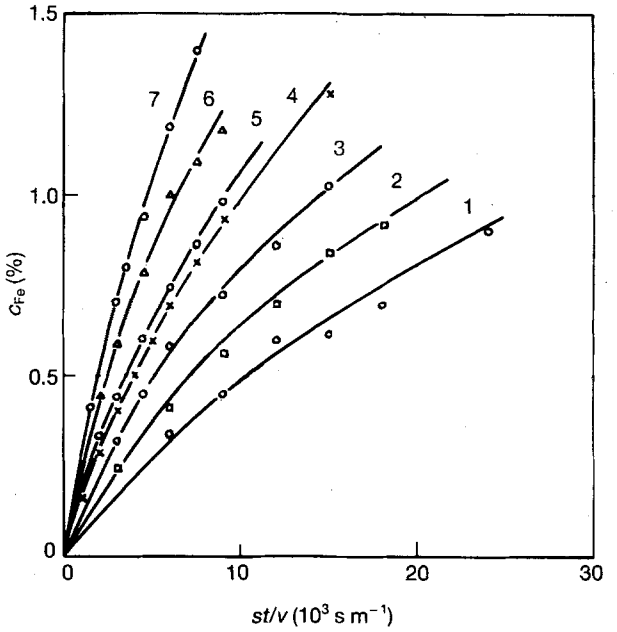

Figure 6 Concentration of iron from a 50% Fe–50% Ni alloy in liquid aluminium plotted against st/v, for temperature = 700 °C, s/v = 10 m^{-1}, and rotational speeds, (1) 6.45, (2) 9.00, (3) 15.3; (4) 24.0, (5) 32.7, (6) 54.0, and (7) 82.4 rad s^{-1}.

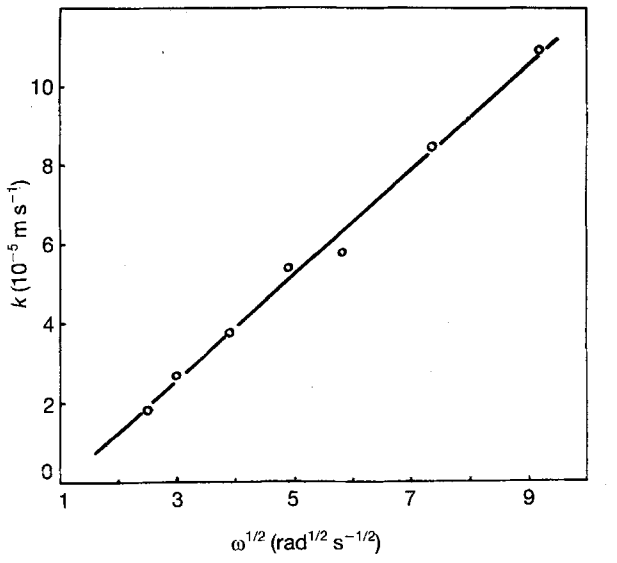

Figure 7 A plot of k against $\omega^{1/2}$ at $c_{Fe} = c_{Ni} = 0.7\%$, for temperature 700 °C, and a 50% Fe–50% Ni alloy.

and nickel additions and the large scatter in viscosity values even for pure liquid aluminium. This was solved in the simplest possible manner; the viscosity was adopted as 4.8×10^{-7} m^2 s^{-1} (see [1]) for all the aluminium melts. In view of a few times scatter in viscosity values of pure aluminium, this approximation does not seem too rough.

The second problem was connected with a change in k-values with increasing iron and nickel concentrations in the aluminium melt. To make a comparison possible, all calculations were performed using k-values at $t = 300$ s and $t = 1500$ s.

The values of the diffusion coefficients obtained are listed in Table IX. Note that each of these diffusion coefficients is some averaged value for the $c_s/2$ to $(c_s + c)/2$ concentration range which characterizes both iron and nickel diffusion from an Fe–Ni alloy across the diffusion boundary layer into the aluminium melt, since the alloy dissolution is non-selective.

As seen, no definite relationship can be revealed between the composition of Fe–Ni alloys and the value of the diffusion coefficient. It should only be noted that, firstly, in the case of a 90% Fe–10% Ni alloy its value apparently tends, with increasing iron concentration in the melt, to the value, $D_{Fe} = 1.24 \times 10^{-9}$ m^2 s^{-1} [9], of the diffusion coefficient of pure iron in liquid aluminium at 700 °C, as might be anticipated. Secondly, the other values are less than or close to the diffusion coefficient of pure nickel in liquid aluminium which is reported as $D_{Ni} = 2.7 \times 10^{-9}$ m^2 s^{-1} [10] or 3.86×10^{-9} m^2 s^{-1} [11]. Thirdly, a somewhat greater value of D for a 25% Fe–75% Ni alloy might be connected with its solid-state ordering [2, 3].

3.6. Estimation of the dissolved part of the solid base

In practice, it is often necessary to know not only the concentration of the dissolved material in the liquid bulk but also the thickness of the dissolved part of the solid base as well. The latter can be found using the equation

$$x_{\text{dissolved}} = \frac{c_s v}{\rho s}\left[1 - \exp\left(-\frac{kst}{v}\right)\right] \quad (8)$$

where ρ is the density of the dissolved material (kg m^{-3}). If an alloy containing ψ mass fractions of a given component is being dissolved, then ρ should be replaced by the product $\rho\psi$.

At small times which are typical of technological processes Equation 8 takes the simplest form

$$x_{\text{dissolved}} = c_s kt/\rho \quad (9)$$

This equation can readily be used, for example, to estimate a change in thickness of the solid base during hot-dip aluminizing. If precise values of k are lacking, the dissolution rate constant may be adopted, to the first approximation, as 2×10^{-5} m s^{-1} for little-stirred liquids and 8×10^{-5} m s^{-1} for well-stirred liquids.

4. Conclusion

The dissolution of Fe–Ni alloys containing 90 to 5% Fe in liquid aluminium at 700 °C was found, by the rotating-disc technique, to be non-selective and diffusion controlled.

A strong mutual influence of iron and nickel on their saturation concentration (solubility) in the aluminium melt was observed. It is especially pronounced at Ni contents in initial Fe–Ni alloys exceeding 50%.

Considerable deviations of the concentration–time dependences from the Nernst–Shchukarev equation were revealed for all the alloys investigated. The value of the dissolution rate constant was found to decrease with increasing dipping time and consequently with

TABLE VIII Experimental data on the dissolution kinetics of Fe–Ni alloys of different compositions in liquid aluminium, for temperature = 700 °C, $\omega = 24.0$ rad s^{-1}. $s/v = 10\ m^{-1}$

Content of Fe in alloy (%)	Time (s)	Concentration of elements in aluminium (%)		$\ln [c_s/(c_s - c)]$	k (10^{-5} m s^{-1})
		Fe	Ni		
90	300	0.41	0.040	0.179	5.9
	600	0.66	0.073	0.307	5.1
	600	0.63	0.070	0.290	4.8
	800	0.79	0.090	0.380	4.7
	900	0.75	0.083	0.356	4.0
	1200	0.97	0.11	0.491	4.1
	1400	1.06	0.12	0.551	4.0
	1500	1.11	0.12	0.587	3.9
75	250	0.35	0.12	0.151	6.0
	300	0.39	0.13	0.170	5.6
	600	0.70	0.23	0.329	5.5
	600	0.71	0.24	0.330	5.5
	800	0.89	0.30	0.440	5.5
	800	0.86	0.29	0.422	5.3
	900	0.87	0.29	0.427	4.8
	1000	0.98	0.33	0.498	5.0
	1500	1.30	0.43	0.734	4.8
25	200	0.23	0.68	0.153	7.6
	300	0.32	0.95	0.221	7.4
	400	0.38	1.12	0.265	6.6
	600	0.51	1.53	0.383	6.4
	840	0.65	1.93	0.515	6.1
	900	0.66	1.99	0.535	5.9
	1200	0.81	2.41	0.697	5.8
	1500	0.90	2.69	0.821	5.5
20	300	0.25	1.02	0.193	6.4
	600	0.43	1.74	0.355	5.9
	750	0.51	2.05	0.436	5.8
	900	0.58	2.32	0.511	5.7
	1000	0.62	2.49	0.561	5.6
	1200	0.70	2.78	0.653	5.4
	1400	0.75	2.98	0.721	5.2
15	275	0.19	1.06	0.162	5.9
	300	0.20	1.14	0.175	5.8
	330	0.22	1.26	0.195	5.9
	600	0.36	2.06	0.343	5.7
	900	0.51	2.86	0.515	5.7
	1200	0.60	3.41	0.654	5.5
	1400	0.65	3.65	0.722	5.2
	1500	0.65	3.70	0.736	4.9
10	300	0.17	1.49	0.203	6.8
	600	0.28	2.55	0.378	6.3
	900	0.37	3.32	0.527	5.9
	1200	0.45	4.06	0.695	5.8
	1500	0.50	4.51	0.813	5.4

TABLE IX Diffusion coefficients of the iron and nickel atoms from Fe–Ni alloys across the diffusion boundary layer at the solid–liquid interface into the aluminium melt at 700 °C, $\omega = 24.0$ rad s^{-1}, $\nu = 4.8 \times 10^{-7}\ m^2\ s^{-1}$

Content of Fe in alloy (%)	k (10^{-5} m s^{-1})		D (10^{-9} m^2 s^{-1})	
	At $t = 300$ s	At $t = 1500$ s	At $t = 300$ s	At $t = 1500$ s
90	5.9	3.9	2.4	1.3
75	5.6	4.8	2.3	1.8
50	5.6	4.8	2.3	1.8
25	7.4	5.5	3.2	2.2
20	6.4	5.2	2.6	2.0
15	5.8	4.9	2.4	1.9
10	6.8	5.4	2.9	2.1

increasing the iron and nickel concentrations in the melt. This decrease was typically 20 to 30% in the range 0 to (about) $c_s/2$ of iron or nickel concentration in the bulk of liquid aluminium.

Accordingly, the value of the diffusion coefficient of iron and nickel from Fe–Ni alloys across the diffusion boundary layer into liquid aluminium at 700 °C also decreased with increasing iron and nickel concentration in the melt bulk by about 25 to 40%. In the case of a 90% Fe–10% Ni alloy it tends to the value of the diffusion coefficient of iron from pure iron in liquid aluminium. The other values were less than or close to the value of the diffusion coefficient of nickel from pure nickel in liquid aluminium.

References

1. V. I. DYBKOV, *J. Mater. Sci.* **25** (1990) 3615.
2. M. HANSEN, "Constitution of binary alloys" (McGraw-Hill, New York, 1958) p. 677.
3. A. F. VOL, "Struktura i svoystva binarnikh metallicheskikh system", Vol. I (Fizmatgiz, Moskwa, 1959) p. 782 (in Russian).
4. C. HAYZELDEN and B. CANTOR, *Int. J. Rapid Solidification* **1** (1984–85) 237.
5. K. B. REUTER, D. B. WILLIAMS and J. I. GOLDSTEIN, *Metall. Trans. A* **20** (1989) 719.
6. V. YA. ANOSOV and S. A. POGODIN, "Osnovnie nachala fiziko-khimicheskogo analiza" (Izd-vo Akademii Nauk SSSR, Moskwa-Leningrad, 1947) p. 663 (in Russian).
7. V. G. LEVICH, "Fiziko-khimicheskaya hidrodinamika" (Fizmatgiz, Moskwa, 1959) p. 77 (in Russian).
8. T. F. KASSNER, *J. Electrochem. Soc.* **114** (1967) 689.
9. V. N. YEREMENKO, YA. V. NATANZON and V. I. DYBKOV, *J. Mater. Sci.* **16** (1981) 1748.
10. *Idem. Fiz. khim. Mekh. Mater.* **6** (1981) 3.
11. A. K. ROY and R. P. CHHABRA, *Metall. Trans. A* **19** (1988) 273.

Received 16 June 1992
and accepted 20 April 1993